ACS SENSORS

ACS EDITORS' CHOICE

Article

Cite This: ACS Sens. 2020, 5, 147−153

pubs.acs.org/acssensors

Nanoparticle Reservoirs for Paper-Only Immunosensors

Alejandra Alba-Patiño,[†,‡,§] Cristina Adrover-Jaume,[†,‡,§] and Roberto de la Rica*[,†,‡]

[†]Multidisciplinary Sepsis Group, Balearic Islands Health Research Institute (IdISBa), Son Espases University Hospital, S Building, Carretera de Valldemossa 79, 07120 Palma de Mallorca, Spain

[‡]Department of Chemistry, University of the Balearic Islands, Carretera de Valldemossa km 7.5, 07021 Palma de Mallorca, Spain

Supporting Information

ABSTRACT: Biosensors made entirely of paper are becoming increasingly popular due to their low cost, facile fabrication, and lightweight portability for in-field measurements. However, it is difficult to store nanoparticles in paper substrates without irreversibly binding them to the cellulose matrix. This makes it challenging to fabricate biosensors incorporating nanoparticle probes in paper-based reservoirs. Here, we overcome this limitation with a new method for storing protein-decorated nanoparticles on paper substrates that also allows to release them on demand. It consists of spotting nanoparticles onto pieces of filter paper previously modified with polystyrene sulfonate. Gold nanoparticles modified with avidin or antibodies can be easily transferred from the dry reservoir to a receiving wet piece of paper by simply pressing with the finger or a clamp. Paper-based immunosensors incorporating the reservoir enabled the detection of glycoprotein B from human cytomegalovirus in serum with a limit of detection of 0.03 ng mL^{-1} and a total assay time of only 12 min. The low limit of detection obtained with a short assay time along with the long shelf-life of the reservoirs make the proposed paper-only biosensors ideal of point-of-care diagnostics.

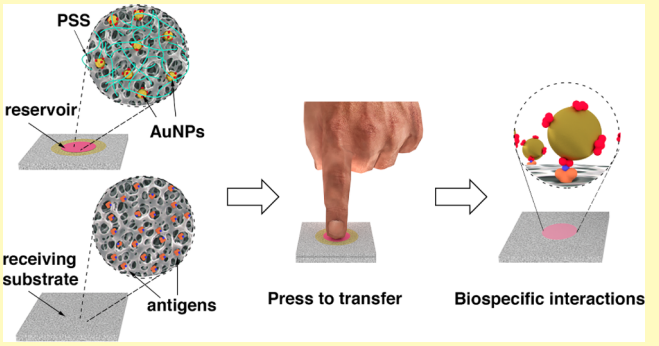

KEYWORDS: *biosensor, origami, gold, colorimetric, plasmonic, paper-based analytical devices, sepsis*

Filter paper is becoming a popular substrate for developing disposable biosensors because of its lightweight, low price, and easy disposal.[1−3] It is commercially available in a wide array of pore sizes and can be easily modified with biomolecules following physical adsorption or covalent attachment methods.[4,5] Its porous matrix can also be used to store reagents such as enzymes and their substrates in order to fabricate reservoirs integrated into paper-based analytical devices.[6] Such reservoirs must preserve the physicochemical properties of the constituent reagents over time while also ensuring an efficient release of their contents to other paper areas upon addition of liquid. Plasmonic nanoparticles are extremely useful building blocks for the fabrication of biosensors using a wide array of signal transduction mechanisms, from colorimetry[7] and surface-enhanced Raman spectroscopy[8] to fluorimetry[9] and electrochemistry.[10] However, plasmonic nanoparticles tend to adsorb irreversibly to paper substrates after drying, which makes it difficult to store them in reservoirs made of this material.[11] Traditionally, this issue has been overcome by making reservoirs out of glass fiber rather than conventional paper.[12] However, this approach is not fully compatible with biosensor designs such as origami paper-based analytical devices. These biosensors are meant to be entirely made of paper with the purpose of simplifying their fabrication and facilitating the contact between the parts without the use of additional adhesives.[13−15] Therefore, it would be desirable to find a method for storing nanoparticles on paper substrates so that they could be implemented in paper-only 3D analytical devices.

In this manuscript, we introduce a new approach for fabricating nanoparticle reservoirs on filter paper. It consists of modifying the paper substrates with the negatively charged polymer polystyrene sulfonate (PSS) in order to avoid the irreversible binding of gold nanoparticles to the cellulose matrix (Figure 1A). Reservoirs prepared this way can release nanoparticles with high efficiency. PSS has been previously used in order to avoid nanoparticle flocculation, usually in the form of alternating layers of PSS and a positively charged polymer such as polydiallyldimethylammonium chloride.[16] It has also been used as a support for growing nanoparticles[17] and for transferring them to a receiving substrate with soft lithography.[18] PSS blended with poly(3,4-ethylenedioxythiophene) is routinely used in order to modify cellulose and render it conductive.[19] In our approach we report a novel use for PSS to avoid the irreversible binding of nanoparticles to cellulose matrices. Besides enabling the release of nanoparticles from cellulose on demand, PSS also makes it possible to transfer nanoparticles from the dry reservoir to a receiving wet paper substrate by simply pressing the former against the latter

Received: October 2, 2019
Accepted: December 18, 2019
Published: December 18, 2019

DOI: 10.1021/acssensors.9b01937
ACS Sens. 2020, 5, 147−153

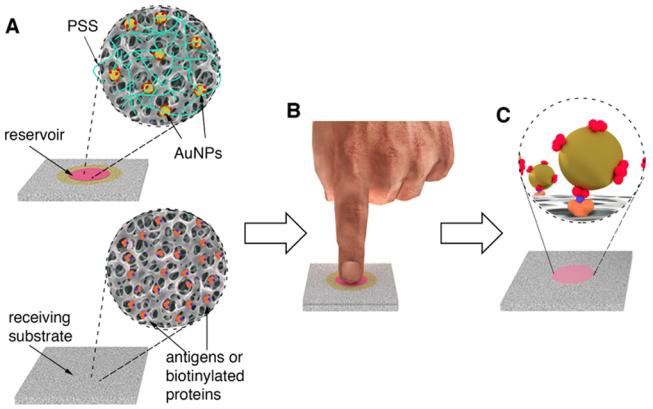

Figure 1. Schematic representation of the paper-based nanoparticle reservoirs and their utilization in biosensing; (A) reservoirs consist of pieces of filter paper modified with PSS and protein-decorated nanoparticles, the receiving paper substrate contains antigens or biotinylated proteins; (B) pressing the dry reservoir onto the wet receiving substrate triggers the transfer of nanoparticles from the former to the latter; (C) the nanoparticles establish biospecific interactions with antigens or biotinylated proteins bound to the receiving paper substrate.

(Figure 1B). This makes the proposed reservoirs useful for developing biosensors with simplified liquid handling schemes because there is no need to add a controlled volume of buffer to the reservoir in order to transfer its contents to a detection area. Furthermore, nanoparticles modified with a protein (avidin, antibodies) retain their ability to specifically recognize their target ligand (biotin, antigens) immobilized on the receiving piece of paper in a dose-dependent manner, which demonstrates the suitability of our approach for developing biosensors (Figure 1C). Vertical transfer between different layers of paper happens efficiently with limited horizontal diffusion without the requirement of hydrophobic barriers[20] or extra additives.[5] This generates intense colorimetric signals due to the biospecific binding of gold nanoparticles to the receiving paper substrate. Our method is an alternative to previously proposed paper-based reservoirs that contained nanoparticles suspended in sucrose-supplemented buffers. The release of nanoparticles from such reservoirs has not been characterized in full,[21] and in some cases, it has been reported to be highly inefficient.[11] The reservoirs proposed here are easy to fabricate, have a long shelf life, and avoid common pitfalls associated to paper biosensors such as the generation of patchy colorimetric signals. The proposed nanoparticle reservoirs were incorporated into immunosensors for the detection of human cytomegalovirus (CMV) in order to demonstrate their suitability for developing biosensors made entirely of filter paper. Our biosensors were able to detect a key antigen of the virus [glycoprotein B (gB) antigen] spiked into serum with a limit of detection of 0.03 ng·mL^{-1} and a rapid assay time within 12 min. To the best of our knowledge this is the lowest limit of detection reported for this analyte thus far, and in a matrix as complex as human serum.[22−24]

EXPERIMENTAL SECTION

Fabrication of Gold Nanoprobes. Citrate-capped gold nanoparticles with a diameter of ca. 40 nm were synthesized with the Turkevich method as previously described.[25] The nanoparticles were then modified with 0.1 mM thiolated polyethylene glycol (PEG) molecules ending in carboxylate moieties [poly(ethylene glycol) 2-mercaptoethyl ether acetic acid, Mn 2100, Sigma] overnight. The resulting pegylated nanoparticles were concentrated and washed with water five times via centrifugation at 8000 rpm for 6 min. The nanoparticles were finally suspended in 0.5 M 2-(*N*-morpholino)-ethanesulfonic acid (Sigma) adjusted at pH 5.5. Carboxylate moieties around the nanoparticles were then transformed into sulfo-NHS esters by adding 1 mg of *N*-(3-dimethylaminopropyl)-*N*′-ethyl-carbodiimide hydrochloride (Sigma) and 2 mg of *N*-hydroxysulfo-succinimide sodium salt (sulfo-NHS, Sigma) for 20 min. Then, the nanoparticles were pelleted by centrifugation, and the supernatant was substituted for a solution containing 1 mg·mL^{-1} avidin in 0.1 M phosphate buffer pH 7.4. After 1 h, unreacted sulfo-NHS esters were capped with 0.1 M glycine and 10 mg·mL^{-1} bovine serum albumin (BSA) for 30 min. The nanoparticles were then washed five times with phosphate buffer saline (PBS) containing 0.1% Tween-20 (PBST). The resulting avidin-covered nanoparticles were kept at 4 °C until used.

Densitometry. Gold nanoparticles on paper substrates generate concentration-dependent colorimetric signals that can be evaluated with densitometry as follows. First, the paper substrates were scanned with an MFC-1910W scanner-printer (Brother). Pixel intensity (PI) profiles were obtained with ImageJ. In grayscale, pure white yields a 255 pixel intensity, whereas pure black yields a 0 pixel intensity. The colorimetric signal S was obtained as follows: First, the pixel intensity in grayscale was measured in a circular area within the area of interest with the Histogram function of ImageJ. The colorimetric signal S was taken as the integer value after subtracting the background signal. Please note that subtracting the background pixel intensity yields inverted signals compared to the raw data.

Fabrication of Nanoparticle Reservoirs. Whatman filter paper number 41, 1, and 6 (pore diameters of 20−25, 11, and 3 μm, respectively) was used. The paper was cut in squares and modified with 50 μL of PSS (30%, Sigma) diluted to different % (v/v) with water when required. After drying, 1 μL of pegylated gold nanoparticles modified with avidin was added and left to dry at room temperature. To study the release of nanoparticles from reservoirs, the nanoparticle-modified dry paper substrates were positioned on top of a folded piece of filter paper and 1 mL of PBST was added three times. The presence of nanoparticles after this step was evaluated by letting the paper dry and measuring any changes in the color of the nanoparticle reservoir with densitometry.

Nanoparticle Transfer and Biorecognition. The transfer of nanoparticles from the reservoir to a receiving paper substrate was studied with the following procedure. Receiving paper substrates were modified with 2 μL of biotinylated BSA (100 μg·mL^{-1} in PBS). Biotinylated BSA was obtained with an EZ-Link sulfo-NHS-biotinylation kit (Thermo Scientific). Control experiments with non-biotinylated BSA were performed in order to assess the contribution of nonspecific interactions to the colorimetric signal. After drying, 1 mL of PBS supplemented with 5 mg·mL^{-1} BSA (PBS−BSA) was added. Then, the reservoir was placed on top of the wet receiving paper and nanoparticle transfer was facilitated by pressing in the center of the spot for 4 min. Subsequently, the reservoir was removed, and the receiving substrate was washed three times with PBST in order to remove nonspecific interactions. After drying, the colorimetric signal was evaluated with densitometry as detailed above.

Detection of gB from CMV. Monoclonal mouse anti-gB (Abcam, ab6499) was biotinylated with an EZ-Link sulfo-NHS-biotinylation kit (Thermo Scientific). Avidin-decorated nanoparticles (100 μL, 72 nM) were incubated with 10 μL of biotinlylated anti-gB for 1 h. After washing three times with PBST, 1 μL of the nanoparticle suspension (140 nM) was spotted on the paper reservoir modified with 30% PSS. The capture antibody (mouse monoclonal anti-gB Abcam ab54023) was spotted on the receiving paper substrate (2.5 μL, diluted 1:100 in PBS) and left to dry at room temperature. Control biosensors were prepared in the same way with anti-*Escherichia coli* (Invitrogen PA1-7213), which does not recognize gB specifically. The resulting paper biosensors were blocked by adding 1 mL of PBS−BSA and letting it dry. To calibrate the biosensors, recombinant gB was spiked into human serum at different final concentrations. After rehydrating the biosensors with 1 mL of PBS−BSA, 50 μL of the spiked serum

DOI: 10.1021/acssensors.9b01937
ACS Sens. 2020, 5, 147−153

samples was added to the receiving paper substrate for 5 min. After washing once with PBST, the reservoir containing nanoparticles decorated with anti-gB was pressed onto the receiving paper with a clamp for 5 min (a photograph of the clamp is available in Figure S5 in the Supporting Information). After 5 min, the reservoir was peeled off and the receiving paper was washed four times with PBST. The colorimetric signal was measured immediately afterward with densitometry as explained above.

RESULTS AND DISCUSSION

In our hypothesis, the modification of paper substrates with PSS facilitates storing nanoparticles in the cellulose matrix while at the same time enabling their release with a high efficiency. This is based on previous studies using PSS to prevent the aggregation of gold nanoparticles via nonspecific interactions.[16] To study this, filter paper was cut in squares, and then, 50 μL of PSS at different % (v/v) was added and left to dry. Three types of paper with different pore sizes (22, 10, and 3 μm) were studied. After drying, substrates with a pore size of 11 and 3 μm were discarded because they were heavily warped and the PSS was unevenly distributed (Figure S1). Paper substrates with a pore size of 22 μm (Whatman #41) remained mostly flat at all PSS concentrations and therefore were subsequently used for the fabrication of nanoparticle reservoirs. They were obtained by pipetting 1 μL of gold nanoparticles in the center of the PSS-modified paper and letting it dry at room temperature. The most widely available gold nanoparticle suspensions are synthesized following the Turkevich method, which renders them capped with negatively charged citrate molecules. To avoid nanoparticle aggregation in solutions containing highly concentrated cations or proteins, citrate molecules are often substituted for thiolated PEG ligands.[26] This not only prevents nanoparticle aggregation but also enables introducing reactive groups such as carboxylate moieties for further covalent attachment with biomolecules. With this in mind, we studied the fabrication of reservoirs containing pegylated nanoparticle probes modified with avidin via amide bond formation. Figure 2A (top row, "before") shows pictures of nanoparticle reservoirs prepared with different % PSS and 72 nM gold nanoparticles modified with avidin. In these images, the spot diameter tends to decrease as the % PSS in the paper increases. Concomitantly, the color intensity increases as the % PSS increases. This can also be observed in the pixel intensity profiles obtained from these images in Figure 2B. In grayscale, the pixel intensity is the highest when the color is white (255) and the lowest when the color is black (0). In Figure 2B, the pixel intensity across the reservoir decreases as the % PSS increases. The spot diameter follows the same trend. This indicates that the nanoparticles are found at higher concentrations and within a smaller volume of the paper matrix as the % PSS increases. We propose that the formation of these smaller and more concentrated nanoparticle reservoirs is related to a slower diffusion of the nanoparticles within the cellulose matrix. It is well established that the viscosity of a solution increases as the concentration of PSS increases.[27] Because the diffusion coefficient is inversely proportional to the viscosity according to the Stokes−Einstein equation, highly concentrated PSS reduces radial diffusion and results in smaller spots containing nanoparticles at a higher concentration. Please note that, although PSS gives a yellowish color to the paper substrate, its contribution to the pixel intensity cannot fully account for the changes in color observed within the reservoir. For example, in Figure 2B, the pixel intensity outside the nanoparticle area decreases from 254 to 234 due to the modification with 30% PSS, but it decreases much more in the center of the reservoir, where the nanoparticles are found (PI ≈ 62). This means that the main contribution to the observed changes in color is a higher concentration of nanoparticles in the reservoir and not the addition of the PSS. In Figure 2B, it is also noticeable that the pixel intensity is lower at the edge of the reservoir than in the center. This is attributed to a higher concentration of nanoparticles at the edge of the spots due to an uneven distribution of solutes during the drying procedure (the so-called "coffee-ring effect").[28] Finally, we sought to determine whether the nanoparticles could be released efficiently from the reservoir, which is an important requirement for integrating reservoirs in biosensors. To this end, 1 mL of PBST was added three times to the reservoirs. In Figure 2A (bottom row, after), the color does not change in reservoirs prepared in the absence of PSS, showing that without the polymer, the nanoparticles are irreversibly bound to the cellulose matrix. However, as the % PSS increases, the color within the spot progressively disappears, which indicates that the nanoparticles exit the reservoir more efficiently when the % PSS in the reservoir is higher. These experiments demonstrate that PSS prevents the formation of irreversible interactions between the nanoparticles and the paper matrix. In Figure 2C, signal quantification with densitometry shows that no color remains in the reservoir when the % PSS utilized to fabricate the reservoir is 15% or higher, which suggests a complete release of avidin-modified nanoparticles under this condition. All in all, the results shown in Figure 2 demonstrate that it is possible to store pegylated nanoparticles modified with proteins in a dry piece of paper previously modified with PSS and that the nanoparticles can be released on demand by simply adding an aqueous solution.

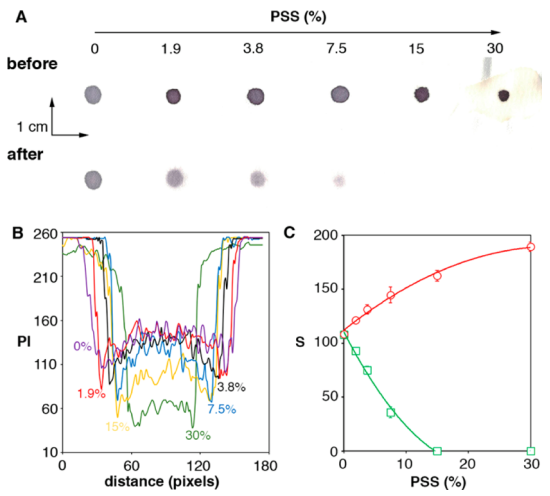

Figure 2. Fabrication of nanoparticle reservoirs with different % PSS; (A) scanned images of the reservoirs before (top row) and after (bottom row) washing three times with 1 mL PBST; (B) pixel intensity (PI) profiles across the reservoirs; (C) colorimetric signal (S) in the reservoir before (red circles) and after (green squares) washing three times with PBST. Error bars are the standard deviation (n = 3). Trend lines are a guide to the eye.

Next, we investigated the impact of nanoparticle concentration in the fabrication of a paper-based reservoir containing avidin-modified gold nanoparticles. To this end, 1 μL of nanoparticles at different concentrations were pipetted onto

DOI: 10.1021/acssensors.9b01937
ACS Sens. 2020, 5, 147−153

paper substrates modified with 30% PSS (Figure 3A). Profile analysis reveals that the formation of a "coffee ring" in the

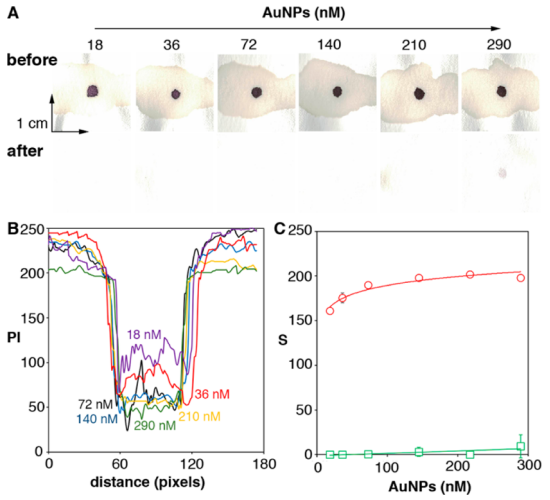

Figure 3. Fabrication of reservoirs with 30% PSS and avidin-decorated nanoparticles at different concentrations; (A) scanned images of the reservoirs before (top row) and after (bottom row) washing three times with 1 mL PBST; (B) pixel intensity (PI) profiles across the reservoirs; (C) colorimetric signal (S) in the reservoir before (red circles) and after (green squares) washing three times with PBST. Error bars are the standard deviation (n = 3). Trend lines are a guide to the eye.

reservoir observed in Figure 2 can be prevented when nanoparticles are dispensed with a concentration of 140 nM or higher because under this condition, the pixel intensity is the same in the center and at the edge of the spot (Figure 3B). It has been proposed that increasing the viscosity of the solution suppresses the formation of coffee rings.[29] In the case under study, the viscosity of the solution increases as the solid volume fraction increases in agreement with the Einstein eq 1

$$\eta = \eta_0\left(1 + \frac{5}{2}\varphi\right) \quad (1)$$

where η is the viscosity of the suspension, η_0 is the viscosity of the dispersion medium, and φ is the solid volume fraction. Therefore, we propose that the increase in viscosity afforded by the higher nanoparticle concentration is a driving force to prevent coffee rings. To study the effect of nanoparticle concentration in the release of contents from the PSS-modified cellulose matrix, the reservoirs were washed with PBST as above and the remaining colorimetric signal was measured with densitometry. In Figure 3A, low row (after) and Figure 3C, the remaining colorimetric signal is very low at all the concentration assayed. Only a slight increase in color can be detected at the highest assayed concentration of nanoparticles. This indicates that 30% PSS is effective at preventing irreversible interactions with the paper even when the reservoirs contain a high concentration of gold nanoparticles. In summary, experiments in Figure 3 indicate that the best fabrication parameters for obtaining reservoirs with the proposed method are 30% PSS and gold nanoparticles with a concentration of 140−210 nM. Under these conditions, nanoparticles within the reservoir are evenly distributed (i.e., there is no coffee ring) and there is a complete release of colloids from the reservoir (no color remains in the paper reservoir).

After studying the best conditions for storing and releasing nanoparticles in cellulose, we tested the ability of transferring the colloids in the dry reservoir to a receiving wet paper by pressing the former onto the latter (Figure 1B). Simultaneously, we tested whether the avidin around the nanoparticles was still able to bind biotinylated molecules in the receiving substrate. In other words, we sought to investigate whether the presence of PSS interfered with our model biological interaction. To carry out this investigation, the dry reservoirs were pressed against a receiving paper substrate modified with biotinylated BSA and saturated with PBST. This transferred liquid from the wet receiving paper to the dry paper reservoir. The resulting rehydration of the reservoir allowed the nanoparticles to be transferred from the reservoir to the receiving substrate. After peeling off the reservoir, the presence of nanoparticles bound to the receiving paper substrate through avidin−biotin interactions was evaluated after washing it three times with PBST. Figure 4A shows images of the

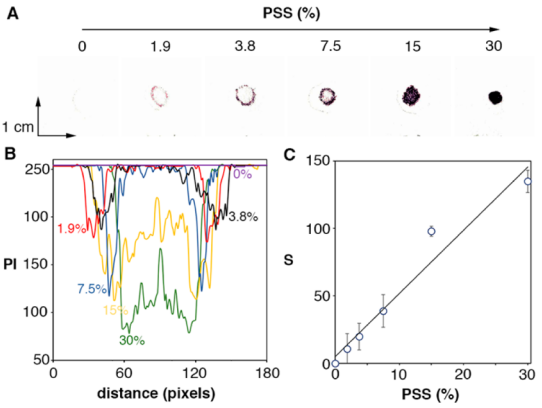

Figure 4. Transfer of avidin-decorated nanoparticles from the reservoirs with different % PSS to receiving substrates modified with biotinylated proteins; (A) scanned images of the receiving substrates after pressing the reservoirs for 4 min, removing them, and washing three times with 1 mL PBST; (B) pixel intensity (PI) profiles across the receiving substrate; (C) colorimetric signal (S) in the receiving paper substrate. Error bars are the standard deviation (n = 3). Trend lines are a guide to the eye.

receiving substrate when the reservoir was made with the same concentration of nanoparticles (72 nM) and different % PSS. In these images, the color in the spot is more homogenously distributed and intense as the % PSS increases. Indeed, at low % PSS, only a nanoparticle ring is generated, which progressively fills up to yield a colored spot at high % PSS. Figure 4B also shows that avidin-decorated nanoparticles tend to accumulate in the periphery of the receiving spot when the concentration of PSS is low. As the % PSS increases, the diameter of the nanoparticle ring decreases and more nanoparticles are observed in the center of the spot. In Figure 4C, the colorimetric signal increases as the % PSS increases because more nanoparticles are transferred within the region of interest. The formation of a ring made of biotin−BSA was ruled out ith the experiment shown in Figure S3, which indicates that the ring is originated by the transfer of the nanoparticles from the reservoir.

We propose two mechanisms for nanoparticle transfer that could result in the formation of a ring. The first mechanism implies that at a low % PSS, nanoparticles diffuse radially and accumulate at the edges upon being transferred, whereas at

DOI: 10.1021/acssensors.9b01937
ACS Sens. 2020, 5, 147−153

high % PSS, the nanoparticles diffuse radially to a lesser extent and are transferred homogenously to the receiving paper. This would result in more concentrated nanoparticles in the center of the spot as the % PSS increases, in agreement with the observations in Figure 4. In the second hypothesis, nanoparticles are transferred preferentially from the edges of the reservoir to the receiving paper substrate, that is, a ring is first generated which subsequently fills up with more nanoparticles. To discern which mechanism governs nanoparticle transfer from the reservoir to the receiving paper, the same experiments were repeated with reservoirs made with the highest concentration of PSS (30%), but with different contact time between paper layers. In Figure 5A,B, the nanoparticles are

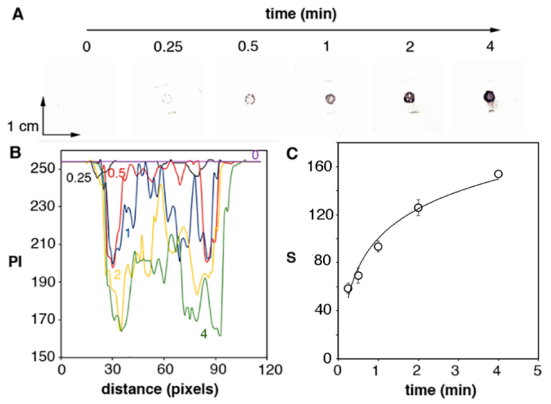

Figure 5. Time-dependent transfer of avidin-decorated nanoparticles from reservoirs containing 30% PSS to receiving substrates modified with biotinylated proteins; (A) scanned images of the receiving substrates after pressing the reservoirs for different times; (B) pixel intensity (PI) profiles and (C) colorimetric signal (S) in the receiving paper substrate. Trend lines are a guide to the eye. Error bars are the standard deviation (n = 3).

transferred as a ring when short transfer times are applied even when the % PSS is high. In Figure 5C, the colorimetric signal increases as the time increases. These results invalidate the first mechanism, since no nanoparticles are observed in the center of the reservoir during the first stages of the transfer process at high % PSS. Therefore, we propose that nanoparticles and PSS are preferentially transferred from the edges of the reservoir. This generates a diffusion barrier that results in the subsequent transfer of polymer and nanomaterials in the central area of the receiving paper, in agreement with the second hypothesis proposed above. Experiments showing the transfer of PSS can be found in Figure S4 in the Supporting Information. Below we study the impact of nanoparticle concentration and paper type in the generation of specific and nonspecific signals for biosensing applications.

Figure 6 shows the effect of the receiving paper pore size in the generation of colorimetric signals when the reservoirs are loaded with 30% PSS and different concentrations of avidin-grafted gold nanoparticles. Nonspecific interactions were evaluated with non-biotinylated (BSA) (control lanes in Figure 6A). Qualitative assessment of Figure 6A shows that using Whatman paper #6 and #1 results in higher colored spots in control experiments compared to Whatman paper #41. This is ascribed to the higher specific area of paper types 6 and 1 because of their smaller pore sizes (3 and 11 μm, respectively), which favors nonspecific interactions between nanoparticles and the receiving substrate. Analysis of the specific signals

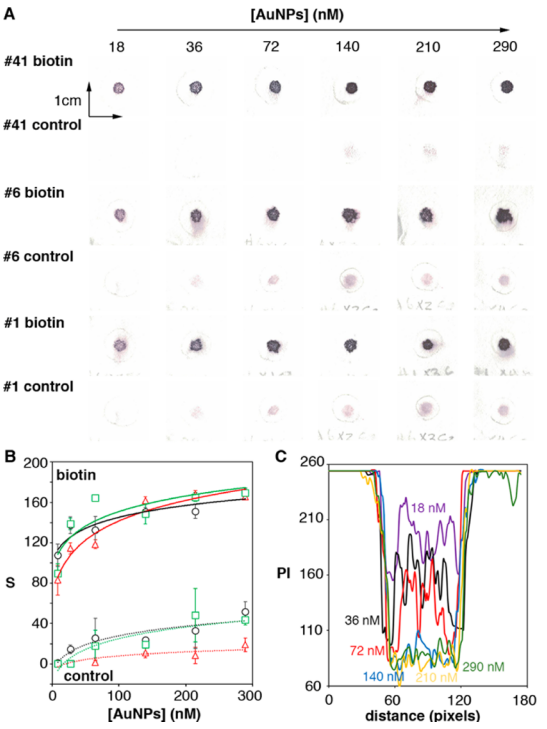

Figure 6. Transfer of avidin-decorated nanoparticles stored at different concentrations to receiving paper substrates with different pore sizes (22, 11, and 3 μm for Whatman Paper 41, 1, and 6, respectively) modified with biotinylated proteins; (A) scanned images of the receiving substrates modified with biotinylated BSA (biotin) or unmodified BSA (control); (B) colorimetric signals in receiving substrates made of Whatman paper #41 (red triangles), #6 (black circles), and #1 (green squares); control experiments with non-biotinylated BSA are indicated with dotted lines; (C) pixel intensity (PI) profiles across receiving substrates made of Whatman paper #41. Error bars are the standard deviation (n = 3). Trend lines are a guide to the eye.

obtained after subtracting the control experiments shows that paper # 41 produces the highest specific signals when using nanoparticles in the concentration range between 140 and 290 nM, whereas paper #1 yields higher specific signals when using nanoparticles in the concentration range between 36 and 72 nM (Figure S7 in the Supporting Information). In Figure 6C, the pixel intensity within the colorimetric signal is homogenously distributed (i.e., no ring formation) when the concentration of nanoparticles in the reservoir is 140 nM or higher and the receiving substrate is Whatman paper #41. These results, in addition to those obtained in Figure 4, indicate that paper-based reservoirs containing 30% PSS and 140 nM nanoparticle probes are the best candidates to generate homogenous and highly intense plasmonic signals in biosensors. The reservoirs were able to establish biospecific interactions even after being kept for a month in an envelope at room temperature (Figure S2). No preservatives were added, and no additional measures such as lyophilization or co-storage with silica gel were taken in order to further preserve the probes, which shows that the proposed method is useful for fabricating biosensors with extended shelf-life without the need to impose strict temperature or humidity storage conditions.

After optimizing the fabrication procedure of the nanoparticle reservoirs, we sought to apply them in sandwich immunoassay for the detection of the antigen gB from CMV. To this end, the avidin-decorated nanoparticles were modified

DOI: 10.1021/acssensors.9b01937
ACS Sens. 2020, 5, 147−153

with biotinylated detection antibodies and stored in the dry paper reservoir as explained above. The receiving paper substrate was modified with capture antibodies and blocked to prevent nonspecific interactions. The immunoassay consisted of adding the target analyte spiked into human serum to the receiving substrate and pressing the paper reservoir for 10 min. After washing away excess reagents, the colorimetric signal was recorded. The whole assay took less than 12 min to be completed. In Figure 7, the proposed paper

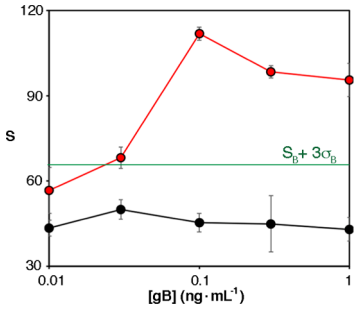

Figure 7. Detection of gB from human CMV in serum with reservoirs containing antibody-decorated nanoparticles and paper substrates modified with anti-gB (red dots) or anti-*E. coli* (black dots) (semilogarithmic scale). S is the colorimetric signal. Error bars are the standard deviation from three independent experiments (n = 3). The green line represents the limit of detection expressed as the blank signal (S_B) and three times the standard deviation of the blank ($3\sigma_B$).

biosensors were able to detect gB with a limit of detection of 0.03 ng·mL^{-1} expressed as the first sample that yielded a signal higher than three times the standard deviation of the blank (green line in Figure 7, 99% confidence). This limit of detection is ca. 100 times lower than the one obtained with a disposable electrochemical biosensor for detecting CMV within 45 min[22] and three times lower than colorimetric ELISA that required several hours to be completed.[23] Control experiments performed with biosensors modified with anti-*E. coli* instead of anti-gB yielded lower nonspecific signals. These results demonstrate that the method for fabricating paper reservoirs containing protein-decorated nanoparticles can be extended to biomolecular interactions other than biotin–avidin interactions, for example, antibody–antigen interactions for developing paper-based immunoassays. It can also be used to store citrate-capped nanoparticles modified with antibodies (Figure S6). Furthermore, the proposed method affords low limits of detection with very short incubation times, which makes it particularly useful for developing rapid diagnostic tests such as those required in decentralized healthcare schemes.

CONCLUSIONS

In conclusion, we have demonstrated that gold nanoparticles modified with PEG and proteins can be stored in filter paper when the substrate is previously treated with PSS. This avoids irreversible interactions with the paper, which enables a complete release of nanoparticles upon addition of an aqueous solution. It also enables transferring the nanoparticles from the reservoir to a receiving substrate by pressing one paper sheet against the other with the finger. Fine-tuning the % PSS avoids the formation of "coffee rings" in both the reservoir and the receiving substrate. This leads to homogenously distributed colorimetric signals resulting from biomolecular interactions between the nanoprobes and substrate-bound molecules. The presence of PSS in the reservoir does not interfere with the generation of avidin–biotin or antibody–antigen interactions and preserves the nanoprobes for at least one month. The best paper types for receiving nanoparticles in paper-only biosensors are #41 when the nanoparticles are stored with a concentration between 140 and 210 nM or #1 when the nanoparticle concentration is 36–72 nM. Nanoparticles decorated with anti-gB were able to detect this analyte with a biosensor made entirely of paper rapidly and with a low limit of detection of 0.03 ng·mL^{-1} (99% confidence). These features make the proposed reservoirs ideal for fabricating paper-only biosensors for point-of-care diagnostics, especially when combined with wax-printed microfluidics.

ASSOCIATED CONTENT

Supporting Information

The Supporting Information is available free of charge at https://pubs.acs.org/doi/10.1021/acssensors.9b01937.

Photographs of filter paper, variation of the colorimetric signal, test for the formation of a "coffee ring", transfer of PSS along with the nanoparticles, pictures of the clamp, detection of mouse IgG with citrate-capped nanoparticles, and specific signal obtained from transfer experiments (PDF)

AUTHOR INFORMATION

Corresponding Author

*E-mail: roberto.delarica@ssib.es.

ORCID

Roberto de la Rica: 0000-0002-5750-1469

Author Contributions

§A.A.-P. and C.A.-J. contributed equally. The manuscript was written through contributions of all authors. All authors have given approval to the final version of the manuscript.

Funding

CTQ2017-82432-R and CTQ2017-92226-EXP.

Notes

The authors declare the following competing financial interest(s): The authors of the paper have filed a patent application (P201930784) in order to protect the intellectual property of some of the discoveries shown in the article.

ACKNOWLEDGMENTS

R.d.l.R. acknowledges financial support from grants FEDER/Ministerio de Ciencia, Innovación y Universidades/Agencia Estatal de Investigación/-Proyecto CTQ2017-82432-R and FEDER/Ministerio de Ciencia, Innovación y Universidades/Agencia Estatal de Investigación/-Proyecto CTQ2017-92226-EXP as well as a Radix fellowship from IdISBa/Impost turisme sostenible/Govern de les Illes Balears. A.A.-P. acknowledges a fellowship for doctoral studies from Roche ("Stop fuga de cerebros" program).

ABBREVIATIONS

PSS, polystyrene sulfonate; AuNPs, gold nanoparticles; gB, glycoprotein B; CMV, cytomegalovirus

REFERENCES

(1) Tenda, K.; van Gerven, B.; Arts, R.; Hiruta, Y.; Merkx, M.; Citterio, D. Paper-Based Antibody Detection Devices Using Bio-

DOI: 10.1021/acssensors.9b01937
ACS Sens. 2020, 5, 147–153

luminescent BRET-Switching Sensor Proteins. *Angew. Chem., Int. Ed.* **2018**, *57*, 15369−15373.
(2) Roig-Sanchez, S.; Jungstedt, E.; Anton-Sales, I.; Malaspina, D. C.; Faraudo, J.; Berglund, L. A.; Laromaine, A.; Roig, A. Nanocellulose Films with Multiple Functional Nanoparticles in Confined Spatial Distribution. *Nanoscale Horiz.* **2019**, *4*, 634.
(3) Reboud, J.; Xu, G.; Garrett, A.; Adriko, M.; Yang, Z.; Tukahebwa, E. M.; Rowell, C.; Cooper, J. M. Paper-Based Microfluidics for DNA Diagnostics of Malaria in Low Resource Underserved Rural Communities. *Proc. Natl. Acad. Sci. U.S.A.* **2019**, *116*, 4834−4842.
(4) Wang, S.; Ge, L.; Song, X.; Yan, M.; Ge, S.; Yu, J.; Zeng, F. Simple and Covalent Fabrication of a Paper Device and Its Application in Sensitive Chemiluminescence Immunoassay. *Analyst* **2012**, *137*, 3821.
(5) Chu, W.; Chen, Y.; Liu, W.; Zhao, M.; Li, H. Paper-Based Chemiluminescence Immunodevice with Temporal Controls of Reagent Transport Technique. *Sens. Actuators, B* **2017**, *250*, 324−332.
(6) Calabria, D.; Caliceti, C.; Zangheri, M.; Mirasoli, M.; Simoni, P.; Roda, A. Smartphone−Based Enzymatic Biosensor for Oral Fluid L-Lactate Detection in One Minute Using Confined Multilayer Paper Reflectometry. *Biosens. Bioelectron.* **2017**, *94*, 124−130.
(7) Russell, S. M.; de la Rica, R. Paper Transducers to Detect Plasmon Variations in Colorimetric Nanoparticle Biosensors. *Sens. Actuators, B* **2018**, *270*, 327−332.
(8) Catala, C.; Mir-Simon, B.; Feng, X.; Cardozo, C.; Pazos-Perez, N.; Pazos, E.; Gómez-de Pedro, S.; Guerrini, L.; Soriano, A.; Vila, J.; et al. Online SERS Quantification of Staphylococcus Aureus and the Application to Diagnostics in Human Fluids. *Adv. Mater. Technol.* **2016**, *1*, 11600163.
(9) Ellairaja, S.; Krithiga, N.; Ponmariappan, S.; Vasantha, V. S. Novel Pyrimidine Tagged Silver Nanoparticle Based Fluorescent Immunoassay for the Detection of Pseudomonas Aeruginosa. *J. Agric. Food Chem.* **2017**, *65*, 1802−1812.
(10) Liang, B.; Zhu, Q.; Fang, L.; Cao, Q.; Liang, X.; Ye, X. An Origami Paper Device for Complete Elimination of Interferents in Enzymatic Electrochemical Biosensors. *Electrochem. Commun.* **2017**, *82*, 43−46.
(11) Ruivo, S.; Azevedo, A. M.; Prazeres, D. M. F. Colorimetric Detection of D-Dimer in a Paper-Based Immunodetection Device. *Anal. Biochem.* **2017**, *538*, 5−12.
(12) Deraney, R. N.; Mace, C. R.; Rolland, J. P.; Schonhorn, J. E. Multiplexed, Patterned-Paper Immunoassay for Detection of Malaria and Dengue Fever. *Anal. Chem.* **2016**, *88*, 6161−6165.
(13) Liu, H.; Crooks, R. M. Three-Dimensional Paper Microfluidic Devices Assembled Using the Principles of Origami. *J. Am. Chem. Soc.* **2011**, *133*, 17564−17566.
(14) Liu, H.; Xiang, Y.; Lu, Y.; Crooks, R. M. Aptamer-Based Origami Paper Analytical Device for Electrochemical Detection of Adenosine. *Angew. Chem., Int. Ed.* **2012**, *51*, 6925−6928.
(15) Kim, H. J.; Kwon, C.; Noh, H. Paper-Based Diagnostic System Facilitating Escherichia Coli Assessments by Duplex Coloration. *ACS Sens.* **2019**, *4*, 2435−2441.
(16) McLintock, A.; Cunha-Matos, C. A.; Zagnoni, M.; Millington, O. R.; Wark, A. W. Universal Surface-Enhanced Raman Tags: Individual Nanorods for Measurements from the Visible to the Infrared (514-1064 Nm). *ACS Nano* **2014**, *8*, 8600−8609.
(17) Cai, W.; Wang, W.; Lu, L.; Chen, T. Coating Sulfonated Polystyrene Microspheres with Highly Dense Gold Nanoparticle Shell for SERS Application. *Colloid Polym. Sci.* **2013**, *291*, 2023−2029.
(18) Basarir, F. Fabrication of Gold Patterns via Multilayer Transfer Printing and Electroless Plating. *ACS Appl. Mater. Interfaces* **2012**, *4*, 1324−1329.
(19) Khan, S.; Ul-Islam, M.; Ullah, M. W.; Israr, M.; Jang, J. H.; Park, J. K. Nano-Gold Assisted Highly Conducting and Biocompatible Bacterial Cellulose-PEDOT:PSS Films for Biology-Device Interface Applications. *Int. J. Biol. Macromol.* **2018**, *107*, 865−873.
(20) Choi, S.; Kim, S.-K.; Lee, G.-J.; Park, H.-K. Paper-Based 3D Microfluidic Device for Multiple Bioassays. *Sens. Actuators, B* **2015**, *219*, 245−250.
(21) Chen, C.-A.; Yeh, W.-S.; Tsai, T.-T.; Li, Y.-D.; Chen, C.-F. Three-Dimensional Origami Paper-Based Device for Portable Immunoassay Applications. *Lab Chip* **2019**, *19*, 598−607.
(22) Pires, F.; Silva, H.; Domínguez-Renedo, O.; Alonso-Lomillo, M. A.; Arcos-Martínez, M. J.; Dias-Cabral, A. C. Disposable Immunosensor for Human Cytomegalovirus Glycoprotein B Detection. *Talanta* **2015**, *136*, 42−46.
(23) Pires, F.; Arcos-Martinez, M. J.; Dias-Cabral, A. C.; Vidal, J. C.; Castillo, J. R. A Rapid Magnetic Particle-Based Enzyme Immunoassay for Human Cytomegalovirus Glycoprotein B Quantification. *J. Pharm. Biomed. Anal.* **2018**, *156*, 372−378.
(24) Susmel, S.; O'Sullivan, C. K.; Guilbault, G. G. Human Cytomegalovirus Detection by a Quartz Crystal Microbalance Immunosensor. *Enzyme Microb. Technol.* **2000**, *27*, 639−645.
(25) Russell, S. M.; Doménech-Sánchez, A.; de la Rica, R. Augmented Reality for Real-Time Detection and Interpretation of Colorimetric Signals Generated by Paper-Based Biosensors. *ACS Sens.* **2017**, *2*, 848−853.
(26) de la Rica, R.; Aili, D.; Stevens, M. M. Enzyme-Responsive Nanoparticles for Drug Release and Diagnostics. *Adv. Drug Delivery Rev.* **2012**, *64*, 967−978.
(27) Boris, D. C.; Colby, R. H. Rheology of Sulfonated Polystyrene Solutions. *Macromolecules* **1998**, *31*, 5746−5755.
(28) Zhang, D.; Gao, B.; Chen, Y.; Liu, H. Converting Colour to Length Based on the Coffee-Ring Effect for Quantitative Immunoassays Using a Ruler as Readout. *Lab Chip* **2018**, *18*, 271−275.
(29) Cui, L.; Zhang, J.; Zhang, X.; Huang, L.; Wang, Z.; Li, Y.; Gao, H.; Zhu, S.; Wang, T.; Yang, B. Suppression of the Coffee Ring Effect by Hydrosoluble Polymer Additives. *ACS Appl. Mater. Interfaces* **2012**, *4*, 2775−2780.

DOI: 10.1021/acssensors.9b01937
ACS Sens. 2020, 5, 147−153